Automated Evaluation of Surface Roughness using Machine Vision based Intelligent Systems

Varun Chebrolu[1,2], Ramji Koona[1] & R S Umamaheswara Raju[2]*

[1]A U College of Engineering (A), Andhra University, Visakhapatnam 530 003, Andhra Pradesh, India

[2]Department of Mechanical Engineering, MVGRCE(A), Vizianagaram 535 005, Andhra Pradesh, India

Machine vision systems play a vital role in entirely automating the evaluation of surface roughness due to the hitches in the conformist system. Machine vision systems significantly abridged the ideal time and human errors for evaluation of the surface roughness in a nondestructive way. In this work, face milling operations are performed on aluminum and a total of 60 diverse cutting experiments are conducted. Surface images of machined components are captured for the development of machine vision systems. Images captured are processed for texture features namely RGB (Red Green Blue), GLCM (Grey Level Co-occurrence Matrix) and an advanced wavelet known as curvelet transforms. Curvelet transforms are developed to study the curved textured lines present in the captured images and this module is capable to unite the discontinuous curved lines present in images. The CNC machined components consists of visible lay patterns in the curved form, so this novel machine vision technique is developed to identify the texture well over the other two extensively researched methods. Artificial Neural Network-Particle Swarm Optimization (ANN-PSO) intelligent models are developed to evaluate the surface roughness from texture features. The model average error attained using RGB, GLCM, Curvelet transform-based machine vision systems are 12.68, 7.8 and 3.57 respectively. In comparison, the results proved that computer vision system based on curvelet transforms outperformed the other two existing systems. This curvelet based machine vision system can be used for the evaluation of surface roughness. Here, image processing might be crucial in identifying certain information. One crucial issue is that, even as performance improves, cameras continue to get smaller and more affordable. The possibility for new applications in Industry 4.0 is made possible by this technological advancement and the promise of ever-expanding networking.

Keywords: ANN-PSO, Curvelet transforms, GLCM, Industry 4.0, RGB, Surface roughness evaluation

Introduction

Major impetus of manufacturing plant is to prepare workpieces with precise tolerances for dimensions, surface quality and shape. Current manufacturing industries conservatively measure surface roughness using instruments with diamond-tipped probes. The foremost hitch with the contemporary instrument is the manual method of measurement. Such instruments require human interventions, efforts, time-consuming and even form scratches on the machined surfaces. Automation of the surface texture measuring process is a tough task in the manufacturing industry. Equipment like Optical instruments, interferometers and microscopes are used by several researchers to overcome the aforementioned problems. This work suggests a machine vision system for evaluating the roughness of surfaces. The machined component surfaces are captured with a high-resolution industrial camera. Image processing toolbox is used to extract texture features (RGB, GLCM and Curvelet transform) from captured images. ANN-PSO models are developed for the mapping of image texture features and roughness of surface in order to solve the complex problems with minor deviations in data. Biological neural networks serve as the inspiration for a ANN PSO computational tool. The minor deviation data is generated in several applications like process control, facial recognition, medical investigations etc. As a powerful tool ANN is used to train the multi-input data to form the constrains developed by PSO. Automation of surface roughness measurement is a difficult task. Surface roughness is the curved shape irregularity brought about by the cutting instrument on the workpiece. The new study that used curvelet transformations to investigate curved forms on machined components established the field of study. An intelligent machine vision system thus developed is used for the evaluation of surface roughness. Industry 4.0 relies heavily on imaging applications

———————
*Author for Correspondence
E-mail: maheshraju@mvgrce.edu.in

and developed system as such will be of greater use for machining industry.

Review of Literature

Review of Progress on Machine Vision Systems

The Artificial Neural Network (ANN) is an efficient tool for surface roughness prediction in machining processes. Based on the trial-and-error method, the number of hidden layers and nodes are determined to give a good prediction of surface roughness using the number of training samples and the ANN training algorithm.[1] AISI 1040 and Aluminium alloy 5083 materials are used for face milling. The surface detection is made possible by the Neural Network Model (NNM) for the data acquired from the conversion of binary images of machined surface and surface roughness.[2] A mixed variable approach (vibration signature and true color) of the machined surfaces is used for the estimation of the surface texture. Support Vector Machine (SVM) a forward mapping regression tool is used for estimation of the surface texture.[3] The surface roughness characterization is done for end milled components with the help of machine vision and ANN. model is developed between the major peaks based on cutting parameters and grey level for roughness estimation.[4]

Roughness is estimated by comparing it with known surface roughness from Database. Machined samples are examined by the light interferometer; analyzing and comparing three regression models with each other by estimating the parameters of the cutting, roughness can be estimated. The obtained results found that the random forest regression model is much superior to multiple regression models for surface roughness prediction.[5] A non-contact type Machine Vision System (MVS) is developed for end-milled components machined at diverse cutting parameters.[6]

The roughness of a machined component is measured by a stylus probe instrument. The images of the machined components are captured and grey level co-occurrence matrixes are extracted to map roughness features to image textures. The mapping and estimation of roughness are done using ANN method. Qualitative and quantitative evaluation of surface texture, calibration of inspected surfaces is performed on end milled metals. By using the roughness parameters, comparison is done between contact and vision based measurements. Surface roughness is estimated by the cusp lines and tool marks on machined surfaces under optimal cutting conditions. Vision-based system has a 10% accuracy than stylus-based measurement.[7] The surface roughness of specimen has an impact on the performance of the machined parts. Roughness is evaluated by the vision system by capturing images of the tool tip and simulation is performed to the surface profile in finish turning. The algorithm detects the machining condition of the simulated images and results successfully showed that this method is used as an indicator of tooltip quality in finish lathe machining. The final surface profile is forecasted to control the performance of the product by using this method.[8] The grinding operation is performed on a stainless steel grade 316 L with a depth of cut of 0.1 mm. Mitutoyo surf-test equipment is used to measure the surface roughness of the components which are machined. Frame buffers are used to transfer data to the workstation. The acquisition of images is accomplished using MATLAB image acquisition software for greyscale level in the RGB image of the workpiece. The distance between the scratches is measured by a measuring tool and used for characterization of the machine surfaces. This investigation avoided direct contact with the surface, helped to analyze the textured surface and improved the accuracy.[9] The processes such as end milling, horizontal/vertical milling and the shaping operations are performed for the identification of machined surfaces using digital image processing. In his work, an automated system that is capable of classifying machined plates is developed. It tests calibrated machined plates of all three types in MATLAB software. This process requires a metallurgical microscope of reasonable magnification for analysis. The Automated classification method finds Accuracy and repeatability. The Average error percentage is calculated. To simplify the technique a Graphical User Interface (GUI) is developed in MATLAB.[10]

Review of Progress on RGB

They developed a correlation of different metal parts using RGB images. The color spectrum of RGB images identifies the surface of the metal parts and then it obtains the expressions of covariance functions. The coefficient values of RGB images are analyzed by evaluation of pixel images. Ten-point average roughnesses are considered. The surface profile is moved repeatedly on the small trace with some speed and depth. The values of the correlation coefficient are changed to the correlation matrix and

estimated. Four sample images are taken to find the surface roughness. Two computer programs SURFCOR_M and PCOR_M by MATLAB software is used for calculations. Covariance functions are varied by the quality of the surfaces. Taking RGB colors average correlation coefficient is obtained.[11] Grinding operation is performed and surface roughness is evaluated based on the sharpness of the machined component surface image. A correlation algorithm is developed between the RGB image sharpness and the surface roughness. Images are analyzed at Constant and varying illuminations in the developed correlation algorithm model. The experimentation is performed on 32 samples with dimensions 50 × 50 mm is machined on a hand-feed grinding machine on a HR-618S and a curve graph is plotted to validate the surface roughness. Nine different positions are selected to test the roughness and to improve the accuracy. This shows that the smaller the roughness, the larger be the sharpness of virtual images.[12]

This method justifies the HVS and gives information that clear images have small roughness and blurred images have large roughness. This is a new method to improve the mathematical model for roughness measurement. In this method, surface type classification based on type of surface images by varying lightened surfaces is improved. The inspection of surface types is performed in a dark environment with the help of a directional light source to illuminate the surface. This light source and its relative position can be expected using a light reference model using which diffused reflectance values are calculated for each RGB color channel. The surface type data is collected by attaching a light source to an RGB depth sensor. The diffused reflectance of trained classifier values achieved higher accuracy in classification rather than the RGB values of the trained classifier. Accuracy of 90% is attained in a single surface plane whereas diffused reflectance values in multiple surface planes over RGB attained an accuracy of 49.24% and 13.66% respectively.[13]

Review of Progress on GLCM

A machine vision system is developed at different ambient light conditions for measurement of surface roughness of 38 mm diametric grounded components. The Gray level co-occurrence matrix is used to find the effect of light in ambient condition on grounded workpieces. A new method is developed between the ambient light and image texture features at an

intensity l to improve the surface roughness. This method finds the real roughness by considering the mean gray level value. The proposed method showed more accurate surface roughness than the gray level co-occurrence matrix when the error is set at 0.05 μm between a value for inspecting and its actual real surface roughness.[14] A system based on machine vision is developed for C–50 steel workpiece material in the dry cutting conditions of turning operation. GLCM technique is used to analyze images of machining surfaces captured by cameras. GLCM technique depends on the appropriate values of Pixel Pair Spacing (PPS). i and j values of GLCM matrix can be determined by counting the number of occurrences of pixel pairs at a specified distance or direction. The orientation of workpiece is set at 30°. Image processing is performed in MATLAB® (version7.8.0.347 R2009a). The average surface roughness (Ra) of the turned surfaces is measured. Contrast and homogeneity are the texture features used to study the tool monitoring, variations in machining time, roughness of the surface and wear of the tool at two different feed rates from GLCM. Contrast is the best parameter in turning for tool condition monitoring.[15] A turning operation is performed to find the roughness of surface using features of image texture. Texture features are used to measure the surface roughness of the captured images produced by a vision system. The surface roughness of machined workpiece is estimated by GLCM. Features of each texture and their arithmetic average height (Ra) of the correlation coefficient is calculated. GLCMTF (GLCM texture features) an image analysis software program is used to analyze captured images. Six texture features like Sum entropy (SENT), Sum variance (SVAR), Angular second moment (ASM), Difference average (DVAR), Sum average (SAVR) and Cluster shade (CSH) are highly interconnected with Ra. There was a maximum error rate of 7% between the actual Ra and the estimated Ra.[16] The face milling procedure is carried out on AA6060 to find the surface roughness using digital image features. Surface roughness is generated by using an adaptive Neuro-fuzzy inference system (ANFIS). A new online system is made by using the input parameters depth of cut, spindle speed, feed by mixed factorial design to find the surface roughness. Standard greyscale deviation and mean greyscale values of entropy and all the digital image matrix members digital image greyscale matrix are studied and discussed. A database is created using the surface

measurements from the obtained input results and generation of roughness is predicted using ANFIS. Extracting features from digital images and the real values are compared with the built online system normalized root mean square error (NRMSE) or assessing error. Thus assessing the error obtained is 6.98% from the machined surfaces.[17]

Review of Progress on Curvelet Transforms

A CNN (Convolutional Neural Network) method is used in estimating the surface roughness intelligently. The features employed include intelligent neural network learning, texture skew correction, and image filtering. Surface topology data are obtained using the dual-tree complex wavelet transform in two dimensions. Residual network recognises the filtered features. To measure the surface roughness, cast iron made of is chosen as a material. Testing results ensure having higher precision surface roughness.[18] Surface roughness is computed utilising a hybrid algorithm's time series analysis, contact technique variations, and wavelet transform. The use of Lyapunov experiment parameters in various processes allows for the recognition of surface dynamic features. Image entropy in the machining processes like milling and turning specifies the length of the image. The machining process can minimise image noise and eliminate image curvature caused by the reflection of light. Comparing and evaluating the dynamic properties of surfaces using contact and non-contact techniques. Estimated roughness has shown accurate roughness with the measured surface roughness.[19] Images combine straight lines with curves. In order to express the edges along the lines and singularities in a material, curvelet transform is used. Here, curvelet transforms are used to examine the texture categorization. One group feature vector is created and stored in a curvelet database using the curvelet numerical features, for instance, the mean and standard deviation. The datasets for wavelet and ridgelet transforms are then compared to this database, and curvelet transform shown superior accuracy due to the sparse representation of images.[20] This article describes a machine vision system that uses texture data from curvelet transforms to estimate surface roughness. Software called MATLAB is used to process the photos. By using the RGB information in the image, a face milling is carried out, followed by the extraction of features. The surface grinding process is carried out at different depths of cut by maintaining constant speed and feed. On mild steel plates, sholder milling and face milling operations are carried out, and

curvelet transforms are taken into account along with Standard Deviation (STD), Median, Mean, Mode, and entropy. An intelligent system based on machine vision roughness valuation method maps the texture features using the algorithm which uses the method of Flower Pollination (FPA) to accurately evaluation the surface roughness value. By comparing the results of FPA and SVM, surface roughness is assessed. Average errors of these two methods are 17.49% and 4.94%. When dealing with limited amounts of data, the FPA model outperformed the SVM model.[21] Estimated machining performance is displayed along with the machining procedures. After image processing in MATLAB, data extraction is carried out using the curvelet transform on a surface image as the input data. A typical vertical machining centre is used for face and shoulder milling operations. Considerations for measuring roughness include mean, median, mode, and entropy. The curvelet data is utilised in the creation of front-end software. The curvelet data is discretized using the Un-equally Spaced Fast Fourier Transform technique. The curvelet data is classified using an SVM model, and this calculates the roughness of machined surfaceand anticipated values. Shows the operational procedure and machining performance and is used for inspection in automation.[22]

Several researchers developed machine vision systems based on RGB and GLCM. Curvelet transforms-based models to estimate the roughness as mentioned in the above literature review are very rare. This gap in research provided scope for the development of an intelligent machine vision systems for surface roughness evaluation. In this work, an attempt has been made by performing 60 diverse experiments and an ANN-PSO-based surface roughness estimation systems are developed using the texture features namely RGB, GLCM and Curvelet transform. ANN-PSO models are developed to map the image processing data and surface finish. The two are contrasted with the ANN-PSO estimated average error percentage of the above mentioned techniques. Developed image processing techniques and ANN-PSO models to estimate the surface roughness. By iterating to produce the quality measure, the ANN-PSO model provides the best possible result.

Experimental Procedure

Using Design Expert, a Design of Experiments (DOE) programme, the order of 60 different CNC face milling tests are generated. DOE selects the most

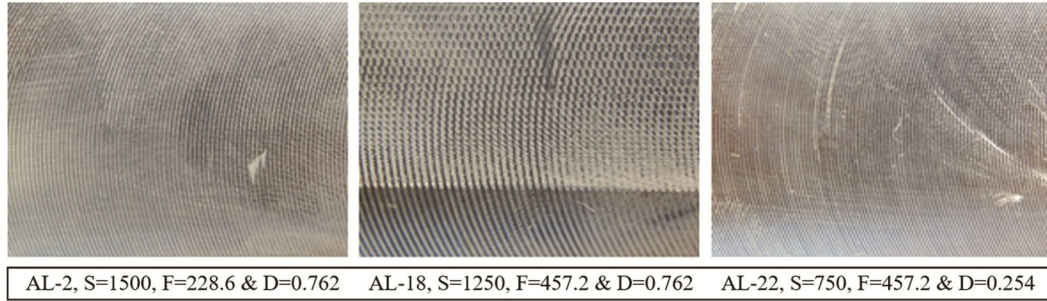| AL-2, S=1500, F=228.6 & D=0.762 | AL-18, S=1250, F=457.2 & D=0.762 | AL-22, S=750, F=457.2 & D=0.254 |

Fig. 1 — Surface Images of the machined component at diverse cutting conditions

advantageous trend of trials that can be carried out under statistically perfect conditions. The cutting parameters for the face milling process are chosen to be four different speeds, feeds, and depths of cut (see Fig. 1). Speed in rpm, machine feed in mm/min and depth of cut in mm are measured. Aluminum workpieces (AL-1, 2, 3, …, 60) are selected as shown in Fig. 1 for machining. It offers better machinability as a result, which is determined by a number of variables including tool life, surface finish, chip evacuation, material removal rate, and machine-tool power. The machined workpiece images are captured by using SONY DSC-H200 camera by maintaining a fixed gap and are shown in Fig. 1. In a dark room, images are taken to maintain the intensity of light. The capture images are of pixel intensity 5184 × 3888 px, having a resolution of 355 dpi in both vertical and horizontal directions. A classic, high-standard diamond-tipped stylus probe and the Handy Surf equipment are used to measure the surface textures. The arithmetic average value, or Ra, is measured in microns (m), and tables show the corresponding Ra values for each cutting condition.

Image Processing Texture Feature Extraction

A total of 60 diverse face milling operations are performed, high-resolution camera is used to take surface images and surface roughness is measured using a stylus probe instrument. Images that have been captured are processed using tools for image processing like RGB, GLCM and curvelet transform for the generation of texture features.

RGB Texture Feature Extraction

RGB refers to a system for the representation of the color to be used on a computer display. To create any colour in the visible spectrum, R, G, and B are blended in a variety of ratios. R, G, and B levels can each vary from 0% to 100% of maximum intensity. The RGB colour model's primary use is to perceive, represent, and display images in electronic systems.

Colors are represented as RGB values by the Image Processing Toolbox software either directly (in an RGB image) or inferentially (in an indexed image, where the colour map is stored in RGB format).One of the most widespread visual features in image classification is the colour feature. By the percentage of R, G and B in the image, the texture features are extracted to estimate the roughness of the machined surface. The advantages of the image where characteristics of colour include robustness, efficacy, implementation, simplicity, computational ease, and low storage needs. The widely used RGB colour model for digital image processing can be represented as shown in the below Eq. (1),

$$F(x,y) = R(x,y)\vec{r} + G(x,y)\vec{g} + B(x,y)\vec{b} \qquad …(1)$$

where R(x,y), G(x,y), and B(x,y) represent the red, green, and blue values at (x,y), respectively; F(x,y) represents the colour vector at pixel (x,y) of the image; and r, g, and b are unit vectors along the position R, G, and B axes, respectively.

GLCM Texture Feature Extraction

GLCM (Gray-level co-occurrence matrix) is a numerical method of inspecting texture that considers the spatial relationships of pixels, it is also called as the gray-level spatial dependence matrix. The GLCM function describes the texture of an image. It calculates specific values and spatial relationships of pixels in an image and then extracts statistical values of the matrix. The characteristics of the GLCM attributes are homogeneity, contrast, correlation, and energy and the basic equation for calculation and are shown in Eqs 5, 2, 3, 4 respectively.

Contrast is a term used to describe the degree of colour or grayscale distinction between different picture aspects in both analogue and digital images.

$$Contrast = \sum_{n=0}^{G-1} n^2 \left\{ \sum_{i=1}^{G} \sum_{j=1}^{G} P(i,j) \right\}, i-j = n …(2)$$

where, G × G is the number of rows and columns in

the image, the element value of the I row and j column in the matrix is P(i,j).

Moving the template or sub image w around the image region and calculating the value C in that area is the process of correlation.

$$Correlation = \sum_{i=0}^{G-1} \sum_{j=0}^{G-1} \frac{\{i \times j\} \times P(i,j) - \{\mu_x \times \mu_y\}}{\sigma_x \times \sigma_y} \quad \ldots(3)$$

where, μ_x & μ_y are the mean values of j column and i rows respectively and σ_x & σ_y are the standard deviation of j column and i rows respectively

The energy is a measure the localized change of the image.

$$Energy = \sum_{i=0}^{G-1} \sum_{j=0}^{G-1} \{P^2(i,j)\} \qquad \ldots(4)$$

A region of an image's homogeneity is related to the intensity changes that occur there.

$$Homogeneity = \sum_{i=0}^{G-1} \sum_{j=0}^{G-1} \frac{P(i,j)}{1+i-j} \qquad \ldots(5)$$

Curvelet Transforms Texture Features Extraction

Curvelet transforms are an extension to wavelet transforms used to compute the number of straight, curved, angled, and horizontal lines in an image at different scales and angles. The amount of lines in the image is tallied which are curved using curvelet transforms. The purpose of Curvelets is to superimpose a curve on itself of tasks of several dimensions that adhere to the parabolic scaling law. For similar precision, curvelets a smooth contour can be represented with a much smaller coefficient set. A multi-scale geometrical transform known as the curvelet transform indexes units according to their individual direction, scale and positions. A grayscale image with so many edges will benefit from Curvelet Transform, which will record this edge information. As the rotation of tool moves circular, the machined components typically feature surface 'lays' in the curved form. Wavelet transforms are less suitable than this method of counting curves in the image for extraction of features of surface. To reduce the discontinuities present in the curved lines, Candes in the year 2000 developed curvelet transforms. The discontinuities are nosing, blurring and unnatural pixelization present in the pixel array of an image. To rectify the discontinuity in the curved lines, curvelet transforms are used. Wavelet transforms are used to count the number of lines in the horizontal, vertical and slanting directions are counted. Curvelet transforms is an extension to wavelet where the discontinuity in curved lines can be fixed and the curved lines can be

counted easily. Curvelet transforms obey parabolic scaling at a scale of 2-j/2 with ridge length of 2-j/2 and width of 2-j for a given envelope. The curvelet transforms address three main problems over wavelet transforms namely, curve punctuated smoothening is done for the discontinuities in the form by the optimal spare representation of edges. Curvelet transforms have the capability for wave propagation modeling the geometry of the curves. Hamiltonian flow is used to translate the center of the curvelet for wave propagator's optimal sparse representation. Curvelet transforms are mainly used for ill-posed missing data in the curve form and reconstruction. In this work, Unequally Spaced Fast Fourier Transforms (USFFT) are applied as the discrete variant. This uses a devastating rectangular grid along the direction of the curve form to create continuity in the discontinuous cure forms present in an object. The image is uploaded and the obtained curvelet transform data is the mean, standard deviation, entropy, mode and median and the respective Eqs are mentioned below as 6, 7, 8, 9 and 10. Generated texture features are RGB, GLCM and Curvelet transform by image processing. Further PSO algorithm is used to optimize the solution and detailed information of PSO is studied.

Mean (μ) will give you an idea of what pixel color to choose to summarize the color of the complete image.

$$\mu = \frac{1}{n} \sum_{i=1}^{n} x_i \qquad \ldots(6)$$

where, n is the number of pixel values, x represents set of pixel elements

The standard deviation (σ), which measures the dispersion of grey level intensities in images, can also be used to gauge the strength of the alternating signal component that the camera has recorded.

$$\sigma^2 = \frac{1}{n} \sum_{i=1}^{n} (x_i - \mu)^2 \qquad \ldots(7)$$

Entropy is a metric used to determine how many bits are needed to encode image data. The image will be more detailed the higher the entropy value.

$$Entropy = -\sum_{i=0}^{G-1} \sum_{j=1}^{G-1} P(i,j) \times \log(P(i,j)) \qquad \ldots(8)$$

where, G × G is the number of rows and columns in the image & P (i, j) is the element value of i row and j column in matrix

The mode affects both the number of colours that can be displayed in an image and the image's file size.

$$\text{mode} = l + h\left(\frac{f_m - f_1}{2f_m - f_1 - f_2}\right) \qquad \ldots(9)$$

where, l is the lower boundary, h is the size, f_m is the frequency corresponding and f_1 & f_2 are frequency preceding and proceeding to pixel.

The median is determined by inserting the pixel under consideration in place of the middle (median) pixel value after numerically ordering all of the pixel values from the window.

$$Median = L_m + \left[\frac{\frac{n}{2} - F}{f_m}\right]i \qquad \ldots(10)$$

where, n is total frequency, F is cumulative frequency, i is the width and L_m is the lower boundary

Results and Discussion

Model

The weights and biases of neurons are used to build an ANN network. The ANN's initial stage is to create a structure, after which the training of network is done. Biological neural networks in many ways, they are very similar to the brain's processing of information, inspire the ANN competitive tool. A network of artificial neurons that communicate with one another to solve problems is the core of ANN modelling. The ANN network has been trained in this job by PSO. The algorithm is used to train the suggested ANN. The Fig. 2 shows the seven steps that were used to complete the model:
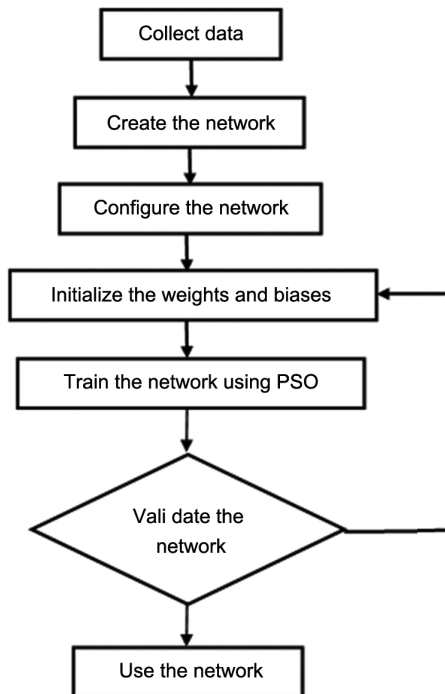

Fig. 2 — Sequential steps of ANN algorithm

PSO is a method of Estimating solutions using artificial intelligence to issues involving numerical maximisation and minimization that are extremely difficult or impossible to solve. JAMES K and R C EBERHART initially described the PSO algorithm in 1995, based on the social behavior of flocking in birds or fish schooling. In order to provide a quality indicator, a computational tool named PSO that iterates to discover the superlative practical elucidation to a problem. By shifting the particles about in the search space, there is a potential solution in the form of a particle. It can look through a lot of potential options while optimizing a problem with fewer resources. Among PSO's there are five core ideas.

Fitness Function Formulation

Data D in the equation… represents a_{11}, a_{12}, a_{13}…….a_n the first input parameter values like RGB% or contrast, correlation, energy and homogeneity in case of GLCM or standard, mean, median, mode, entropy in case of curvelet transforms texture features and R1 in S being corresponding surface roughness value.

$$D = \begin{bmatrix} a_{11} & a_{12} & a_{13} & \cdots & a_{1n} \\ a_{21} & a_{22} & a_{23} & \cdots & a_{2n} \\ \vdots & \vdots & \vdots & \ddots & \vdots \\ a_{N1} & a_{N2} & a_{N3} & \cdots & a_{Nn} \end{bmatrix}, S = \begin{bmatrix} R_1 \\ R_2 \\ \vdots \\ R_N \end{bmatrix} \qquad \ldots(11)$$

Here, N is the total number of experiments and n is the number of design parameters. 'D' matrix refers to input parameters and S is the respective surface roughness. In an attempt to build the model, the corresponding weights (Coefficients) are to be determined. The possible solution weight vector can be written as follows.

$$W = [w_1, w_2, \ldots w_m] \qquad \ldots(12)$$

Here, m refers to the number of weights / coefficients. In the algorithm, the possible set of solutions drawn from the solution space is written as

$$p = \begin{bmatrix} W_1 \\ W_2 \\ \vdots \\ W_p \end{bmatrix} = \begin{bmatrix} w_{11} & w_{12} & \cdots & w_{1m} \\ w_{21} & w_{22} & \cdots & w_{2m} \\ \vdots & \vdots & \ddots & \vdots \\ w_{p1} & w_{p2} & \cdots & w_{pm} \end{bmatrix} \qquad \ldots(13)$$

Here, p refers to population size or number of individuals. While, W_1 is the first individual and the corresponding weight vector is $[w_{11}, w_{12}, \ldots w_{1m}]$

Let the number of iterations in PSO be K, and consider an iteration 't'. In every trial each individual

(weight vector) is taken and inducted into the model along with the data giving the corresponding surface roughness. This obtained surface roughness is the outcome of the model for a set of weights (say W_i) and data (D_i). The surface roughness vector is obtained for this trial which is written as.

$$\hat{R}_{it} = [\hat{R}_{1t}, \hat{R}_{2t}, \dots \hat{R}_{Nt}] \qquad \dots(14)$$

Here, t = 1, 2, . . . k and i = 1, 2, . . . p

Now the fitness corresponding to this trial is computed through the following expression.

$$f_{it} = \frac{\sum_{t=1}^{N} |R_l - \hat{R}_{lt}|}{N} \qquad \dots(15)$$

The fitness vector is

$$f_t = [f_{1t}, f_{2t}, f_{3t}, \dots f_{pt}] \qquad \dots(16)$$

Now, the objective can be written as[23]

$$F(t) = arg_{m=1,\dots p}^{min}[f_{mt}] \qquad \dots(17)$$

ANN-PSO Efficiency

As shown in Fig. 1, image processing is carried out on 60 acquired machined surfaces. The images as shown in Table 1, consisting of red, green, and blue percentages. In the ANN-PSO model, 59 data points are used to map out texture characteristics and surface roughness data. The remaining last information is utilized to evaluate the model's effectiveness, and repeated the process. The measured and predicted values are shown in the Table below. PSO efficiency is mapped once with red, green, blue, and measured roughnesses are factored. The predicted roughness is determined by comparing the input of the image. PSO is used to map texture features to measured surface roughness. Comparing experimentally obtained surface roughness values to those predicted by the model, the overall average error percent of 60 different workpieces is determined. PSO efficiency is estimated below to find the error percentage of RGB.

Regression Plot for Rgb

The blueline represents the fitline and the particles surrounding it are observed to be clustered around the line. This is a sign of positive result and regression value R (0.97117) is also obtained very close to the actual value 1. The multiple regressions are done for a better model to graphically view the proximity of obtained results to the actual one. A regression is a measure of relation between two different variables as shown in Fig. 3 drawn between output and target. The plot shows the maximum of 4% in RGB.

GLCM Trained Dataset

On the 60 machined surfaces that were acquired, image processing is done from the Fig. 1. These images consist of contrast, correlation, energy and homogeneity percentage and the values are shown in Table 2. The 59 data points from a total of 60 texture characteristics where data related to roughness of machined surfaces are mapped using the PSO model. For the rest of the data, this process is repeated before using the additional 1 data to evaluate the model's effectiveness. The measured and anticipated surface roughness values are displayed in the Table. PSO efficiency is mapped after taking into account images' contrast, correlation, energy, homogeneity, and assessed roughness. Predicted roughness is obtained by testing the input of image texture feature. The texture features are mapped with measured surface roughness using PSO. The total average error percentage is computed by comparing the experimental data to the projected surface roughness values predicted by the model for 60 different workpieces. PSO efficiency is estimated below to find the error percentage of GLCM.

Regression Plot for Gray Level Co-Occurrence Matrix

The Multiple regressions are used in this model to (graphically) view the proximity of obtained results to the actual one. The blueline represents the fitline and the particles surrounding it are observed to be clustered around the line. This is a sign of positive result and regression value R (0.98885) is also obtained very close to the actual value 1. A regression is a measure of relation between two different variables. Here is the graph in Fig. 4 drawn between output and target. The plot shows the maximum of 0.69% in GLCM

Curvelet Transform Trained Dataset

The images depicted in Fig. 1 are used to process the images of 60 machined surfaces, which are displayed in Table 3. The 59 data points from a total of 60 texture characteristics where data related to roughness of machined surfaces are mapped using the PSO model. This procedure is carried out again for the remaining data before using the additional 1 data to evaluate the model's effectiveness. The measured and anticipated values are displayed in the Table below. Parameters extracted from image like mean, entropy, mode, median and assessed roughness are taken into account while considering images, and PSO efficiency is mapped. Predicted roughness is

Table 1 — Percentage of Red, Green, Blue, Measured and Predicted surface roughness along with error percentage

Image	R%	G%	B%	Measured	Predicted	Error %
AL-1	33.33	33.84	32.83	3.64	4.33	18.96
AL-2	33.2	33.73	33.07	1.21	1.43	18.18
AL-3	33.39	33.78	32.83	1.1	1.36	23.64
AL-4	33.29	33.57	33.14	4.2	4.46	6.19
AL-5	33.38	33.7	32.92	4	4.01	0.25
AL-6	33.94	33.46	32.6	4.19	5.31	26.73
AL-7	33.42	33.8	32.78	4.67	4.42	5.35
AL-8	33.12	33.92	32.96	4.22	4.55	7.82
AL-9	33.4	33.76	32.85	1.31	1.51	15.27
AL-10	33.18	33.69	33.14	2.24	2.42	8.04
AL-11	33.54	33.48	32.99	1.25	2.71	116.80
AL-12	33.42	33.54	33.04	3.72	3.87	4.03
AL-13	33.69	33.4	32.92	1.14	1.23	7.89
AL-14	33.45	33.79	32.76	2.82	3.27	15.96
AL-15	33.62	33.61	32.77	2.26	2.01	11.06
AL-16	33.85	33.31	32.84	4.65	4.88	4.95
AL-17	33.21	33.79	33	2.62	2.26	13.74
AL-18	33.18	33.75	33.08	4.11	3.88	5.60
AL-19	33.66	33.42	32.92	1.62	1.82	12.35
AL-20	33.61	33.65	32.74	4.05	3.81	5.93
AL-21	33.2	33.77	33.04	4.62	4.56	1.30
AL-22	33.46	33.45	33.09	4.64	4.55	1.94
AL-23	33.28	33.53	33.2	4.27	4.37	2.34
AL-24	33.27	33.59	33.14	4.85	3.88	20.00
AL-25	33.4	33.49	33.1	4.75	4.8	1.05
AL-26	33.32	33.7	32.98	4.36	3.45	20.87
AL-27	33.62	33.55	32.83	1.71	1.56	8.77
AL-28	33.31	33.62	33.07	1.17	1.37	17.09
AL-29	33.52	33.62	32.86	2.52	2.15	14.68
AL-30	33.5	33.71	32.79	2.99	2.79	6.69
AL-31	33.35	33.44	33.21	1.13	1.29	14.16
AL-32	33.28	33.53	33.18	4.28	4.56	6.54
AL-33	33.38	33.7	32.93	2.03	1.92	5.42
AL-34	33.48	33.49	33.03	2.86	2.48	13.29
AL-35	33.4	33.65	32.95	4.37	3.8	13.04
AL-36	33.98	33.37	32.66	2.83	2.33	17.67
AL-37	33.89	33.15	32.96	4.75	4.91	3.37
AL-38	33.65	33.56	32.79	1.69	1.88	11.24
AL-39	33.78	33.41	32.82	4.05	4.15	2.47

(*Contd.*)

Table 1 — Percentage of Red, Green, Blue, Measured and Predicted surface roughness along with error percentage (Contd.)

Image	R%	G%	B%	Measured	Predicted	Error %
AL-40	33.97	33.36	32.68	4.56	4.73	3.73
AL-41	33.39	33.75	32.86	4.42	4.2	4.98
AL-42	33.33	33.55	33.12	1.35	1.71	26.67
AL-43	33.61	33.45	32.94	1.62	1.35	16.67
AL-44	33.25	33.72	33.03	4.14	4.63	11.84
AL-45	33.11	33.74	33.15	3.88	3.73	3.87
AL-46	33.67	33.53	32.8	4.31	3.35	22.27
AL-47	33.48	33.71	32.82	1.17	1.27	8.55
AL-48	33.29	33.69	33.03	2.98	3.1	4.03
AL-49	33.31	33.83	32.87	1.33	1.44	8.27
AL-50	34.33	33.28	32.39	1	1.23	23.00
AL-51	33.35	33.49	33.17	3.26	3.65	11.96
AL-52	33.76	33.31	32.92	4.7	3.98	15.32
AL-53	32.94	33.49	33.57	3.7	3.23	12.70
AL-54	33.34	33.78	32.89	0.97	1.22	25.77
AL-55	33.02	33.48	33.5	4.66	4.77	2.36
AL-56	33.44	33.68	32.88	4.63	4.97	7.34
AL-57	33.74	33.67	32.59	4.19	3.64	13.13
AL-58	33.24	33.79	32.97	1.97	1.92	2.54
AL-59	33.3	33.67	33.03	2.36	2.93	24.15
AL-60	33.39	33.78	32.82	3.43	3.4	0.87
					Average Error:	12.68
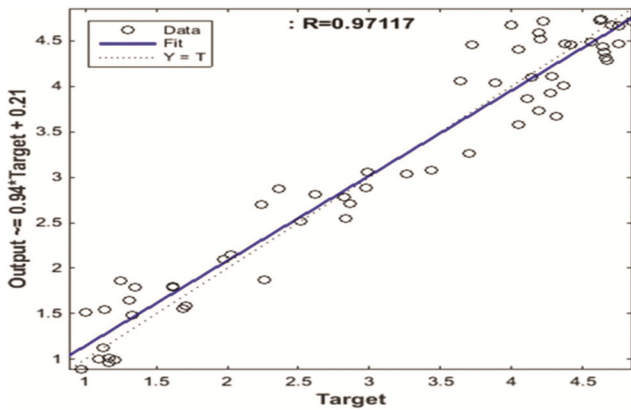
Fig. 3 — Regression plot for RGB

Fig. 4 — Regression plot for GLCM

obtained by testing the input with the last image. The texture features are mapped with measured surface roughness using PSO. Surface roughness values obtained from the experiment are compared with those predicted by the model, and the average error % for all 60 workpieces is computed. PSO efficiency is estimated below to find the error percentage of curvelet transform.

Regression Plot for Curvelet

The Multiple regressions are used in this model to graphically view the proximity of obtained results to the actual one. The blueline represents the fitline and the particles surrounding it and are observed to be clustered around the line. This is a sign of positive result and regression value R (0.9926) is also obtained

Table 2 — Contrast, Correlation, Energy, Homogeneity, Measured and Predicted surface roughness along with error percentage

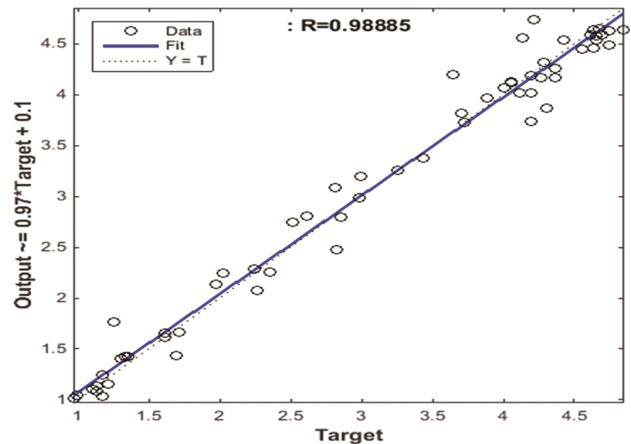| Image	Contrast	Correlation	Energy	Homogeneity	Measured	Predicted	Error %
Al-1	0.4191	0.8472	0.122	0.828	3.64	4.35	19.51
Al-2	0.3219	0.853	0.1529	0.8549	1.21	1.21	0.00
Al-3	0.2907	0.8329	0.1856	0.862	1.1	1.12	1.82
Al-4	0.2474	0.9194	0.1398	0.8855	4.2	4.41	5.00
Al-5	0.3883	0.8862	0.1052	0.8282	4	4.16	4.00
Al-6	0.2722	0.9177	0.1276	0.874	4.19	4.06	3.10
Al-7	0.3216	0.7984	0.1884	0.8554	4.67	3.84	17.77
Al-8	0.2656	0.7442	0.2746	0.8754	4.22	4.33	2.61
Al-9	0.3161	0.8337	0.1666	0.8542	1.31	1.28	2.29
Al-10	0.2225	0.893	0.1835	0.8911	2.24	1.95	12.95
Al-11	0.3064	0.896	0.129	0.8613	1.25	1.92	53.60
Al-12	0.2023	0.9235	0.1653	0.9013	3.72	4.56	22.58
Al-13	0.4363	0..8983	0.0989	0.8259	1.14	1.02	10.53
Al-14	0.2412	0.8649	0.1927	0.8837	2.82	3.14	11.35
Al-15	0.3171	0.8248	0.1767	0.8552	2.26	2.05	9.29
Al-16	0.2845	0.9193	0.1277	0.8716	4.65	4.61	0.86
Al-17	0.2506	0.8499	0.1937	0.8801	2.62	2.59	1.15
Al-18	0.4147	0.8693	0.115	0.8318	4.11	4.25	3.41
Al-19	0.2604	0.8823	0.1718	0.8774	1.62	1.68	3.70
Al-20	0.3094	0.8716	0.1505	0.8593	4.05	4.02	0.74
Al-21	0.3257	0.8265	0.1611	0.8511	4.62	4.51	2.38
Al-22	0.1606	0.9358	0.1896	0.9216	4.64	4.77	2.80
Al-23	0.139	0.9405	0.1933	0.9309	4.27	4.5	5.39
Al-24	0.2568	0.8673	0.1779	0.8776	4.85	4.4	9.28
Al-25	0.3043	0.8775	0.1482	0.8627	4.75	4.63	2.53
Al-26	0.2897	0.8522	0.166	0.8642	4.36	3.96	9.17
Al-27	0.3204	0.8887	0.1271	0.8539	1.71	1.51	11.70
Al-28	0.2757	0.8828	0.1542	0.8697	1.17	1.21	3.42
Al-29	0.2993	0.8669	0.1535	0.8624	2.52	2.65	5.16
Al-30	0.3244	0.8534	0.1495	0.8518	2.99	2.93	2.01
Al-31	0.3076	0.8933	0.1336	0.8599	1.13	1.06	6.19
Al-32	0.413	0.8877	0.1075	0.835	4.28	4.12	3.74
Al-33	0.3416	0.858	0.1377	0.8465	2.03	1.97	2.96
Al-34	0.2961	0.89	0.1351	0.8616	2.86	3.23	12.94
Al-35	0.393	0.888	0.1076	0.8367	4.37	4.09	6.41
Al-36	0.1872	0.9533	0.1374	0.91	2.83	2.84	0.35
Al-37	0.2904	0.9283	0.1253	0.8727	4.75	4.56	4.00
Al-38	0.3118	0.8831	0.1338	0.8574	1.69	2.02	19.53
Al-39	0.1327	0.9485	0.1854	0.935	4.05	3.67	9.38
Al-40	0.162	0.9469	0.1637	0.9211	4.56	4.83	5.92
Al-41	0.2768	0.8475	0.1966	0.8748	4.42	4.23	4.30
Al-42	0.1826	0.9165	0.1885	0.9113	1.35	1.46	8.15
Al-43	0.2962	0.9026	0.1289	0.8634	1.62	1.33	17.90
Al-44	0.3054	0.8459	0.1581	0.8553	4.14	4.43	7.00
Al-45	0.2948	0.8671	0.1597	0.869	3.88	4.22	8.76
Al-46	0.2414	0.895	0.1636	0.8831	4.31	3.84	10.90
Al-47	0.2806	0.8934	0.1447	0.8665	1.17	0.88	24.79
Al-48	0.2244	0.8819	0.1873	0.892	2.98	3.06	2.68

(Contd.)

Table 2 — Contrast, Correlation, Energy, Homogeneity, Measured and Predicted surface roughness along with error percentage (*Contd.*)

Image	Contrast	Correlation	Energy	Homogeneity	Measured	Predicted	Error %
Al-49	0.3528	0.8542	0.1612	0.8499	1.33	1.44	8.27
Al-50	0.2093	0.9485	0.1325	0.9015	1	0.97	3.00
Al-51	0.479	0.8995	0.0888	0.8195	3.26	3.2	1.84
Al-52	0.3684	0.9304	0.0972	0.8484	4.7	4.6	2.13
Al-53	0.0923	0.9621	0.2173	0.9539	3.7	3.48	5.95
Al-54	0.2867	0.7707	0.2287	0.8644	0.97	0.92	5.15
Al-55	0.1241	0.9441	0.2038	0.9328	4.66	4.7	0.86
Al-56	0.3456	0.8605	0.1531	0.8517	4.63	4.76	2.81
Al-57	0.2842	0.92	0.128	0.8727	4.19	3.76	10.26
Al-58	0.2882	0.8834	0.1476	0.8624	1.97	2.49	26.40
Al-59	0.2051	0.9279	0.158	0.8995	2.36	2.43	2.97
Al-60	0.2424	0.9094	0.156	0.8875	3.43	3.61	5.25
			Average error				7.85

Table 3 — Standard, Median, Mean, Mode, Entropy, Measured and Predicted surface roughness along with error percentage

Image	Standard	Median	Mean	Mode	Entropy	Measured	Predicted	Error %
AL-1	166.727	0.5252	2.248	0.0005	6.4172	3.64	4.16	14.29
AL-2	128.712	0.7644	3.57	0.0005	5.6175	1.21	1.22	0.83
AL-3	198.382	0.614	2.402	0.0001	6.279	1.1	1.03	6.36
AL-4	181.629	0.7223	3.714	0.0001	5.8284	4.2	4.12	1.90
AL-5	10.3806	0.8376	4.599	0.0004	5.4911	4	3.94	1.50
AL-6	174.683	0.7363	4.527	0.0003	5.6316	4.19	4.26	1.67
AL-7	145.718	0.8102	3.891	0.0006	5.4688	4.67	4.65	0.43
AL-8	173.09	0.8399	3.816	0.0001	5.5301	4.22	4.74	12.32
AL-9	173.477	0.7574	3.387	0.0003	5.6023	1.31	1.32	0.76
AL-10	161.436	0.7991	3.165	0.0305	5.7097	2.24	2.24	0.00
AL-11	152.956	0.5	2.225	0.0004	6.4741	1.25	1.3	4.00
AL-12	1855327	0.6093	2.418	0.0006	6.1934	3.72	3.72	0.00
AL-13	164.627	0.5464	2.284	5.6414	6.5001	1.14	1.13	0.88
AL-14	183.408	0.8273	3.283	0.0005	5.6448	2.82	2.98	5.67
AL-15	187.327	0.803	3.359	0.0006	5.6931	2.26	2.02	10.62
AL-16	189.648	0.6206	2.475	0.1067	6.237	4.65	4.5	3.23
AL-17	17.9926	0.7613	3.196	0.0002	5.831	2.62	2.83	8.02
AL-18	168.159	1.0446	4.372	0.0004	4.968	4.11	4	2.68
AL-19	171.797	0.9962	3.985	0.0098	5.0756	1.62	1.7	4.94
AL-20	171.349	0.7048	2.888	0.0007	5.9673	4.05	4.06	0.25
AL-21	170.868	0.6068	2.527	0.0002	6.2988	4.62	4.65	0.65
AL-22	131.789	0.6172	3.656	0.0001	5.9451	4.64	4.4	5.17
AL-23	164.67	0.8941	3.436	0.0005	5.3958	4.27	4.28	0.23
AL-24	163.539	0.8115	3.603	0.0006	5.5662	4.85	4.67	3.71
AL-25	171.428	0.7405	3.405	0.0003	5.741	4.75	4.58	3.58
AL-26	157.685	0.7729	3.547	0.001	5.7002	4.36	4.15	4.82
								(*Contd.*)

Table 3 — Standard, Median, Mean, Mode, Entropy, Measured and Predicted surface roughness along with error percentage (*Contd*.)

Image	Standard	Median	Mean	Mode	Entropy	Measured	Predicted	Error %
AL-27	167.491	1.0564	4.349	0.0007	4.9192	1.71	1.72	0.58
AL-28	183.388	0.8442	2.999	0.0007	5.6397	1.17	1.22	4.27
AL-29	162.674	0.6849	3.094	0.0005	5.9665	2.52	2.77	9.92
AL-30	163.164	0.9005	3.834	0.0008	5.4234	2.99	3.08	3.01
AL-31	183.577	0.578	2.583	0.0002	6.3782	1.13	1.04	7.96
AL-32	172.867	0.4534	1.828	0.0003	6.7841	4.28	4.38	2.34
AL-33	168.285	0.6349	2.853	0.0004	6.2074	2.03	2.2	8.37
AL-34	183.174	0.5275	2.148	0.0002	6.5344	2.86	2.81	1.75
AL-35	162.488	0.5227	2.085	0.0002	6.5607	4.37	4.29	1.83
AL-36	129.328	0.4691	2.389	0.0001	6.5351	2.83	2.8	1.06
AL-37	178.736	0.6557	2.663	0.0003	6.1349	4.75	4.7	1.05
AL-38	187.865	0.567	2.372	0.0002	6.3351	1.69	1.58	6.51
AL-39	177.648	0.6942	3.365	0.0181	5.8943	4.05	3.99	1.48
AL-40	179.77	0.5693	2.126	0.0213	6.3943	4.56	4.45	2.41
AL-41	190.609	0.564	2.391	0.0002	6.4125	4.42	4.47	1.13
AL-42	172.929	0.4827	2.072	0.0004	6.5977	1.35	1.43	5.93
AL-43	178.184	0.6569	2.827	0.0003	6.0254	1.62	1.71	5.56
AL-44	180.679	0.6608	3.028	0.0003	6.0248	4.14	4.49	8.45
AL-45	170.068	0.5736	2.465	0.0001	6.4313	3.88	3.94	1.55
AL-46	173.582	0.6682	2.678	0.0003	6.1083	4.31	3.95	8.35
AL-47	177.814	0.8538	3.457	0.0007	5.4876	1.17	1.12	4.27
AL-48	170.028	1.0509	3.773	0.0001	5.0367	2.98	3	0.67
AL-49	141.844	0.4618	1.8	0.0003	6.7301	1.33	1.31	1.50
AL-50	145.594	0.603	2.191	0.0003	6.2977	1	1.02	2.00
AL-51	188.953	0.5666	2.169	0.0002	6.4657	3.26	3.24	0.61
AL-52	175.045	0.5943	2.429	0.0003	6.3552	4.7	4.66	0.85
AL-53	123.469	0.8382	3.35	0.0007	5.541	3.7	3.75	1.35
AL-54	152.378	0.5781	2.04	0.0001	6.4085	0.97	0.94	3.09
AL-55	162.506	0.5276	1.834	0.0159	6.6205	4.66	4.67	0.21
AL-56	147.857	0.7938	3.553	0.001	5.5353	4.63	4.61	0.43
AL-57	149.871	0.563	2.379	0.0003	6.3905	4.19	3.73	10.98
AL-58	135.433	0.3697	1.398	0.0003	6.9452	1.97	2.07	5.08
AL-59	137.25	0.78	3.114	0.0004	5.6962	2.36	2.35	0.42
AL-60	118.328	0.3999	1.414	0.0002	6.8861	3.43	3.45	0.58
				Average error				3.57

very close to the actual value1. A regression is a measure of relation between two different variables. Here is the graph in Fig. 5 drawn between output and target. The plot shows the maximum of 0.25% in curvelet transform.

The processing of captured images for texture features namely RGB, Gray Level Co-occurrence Matrix and Curvelet transform and surface roughness is predicted using ANN-PSO technique. These predicted values are then compared with the
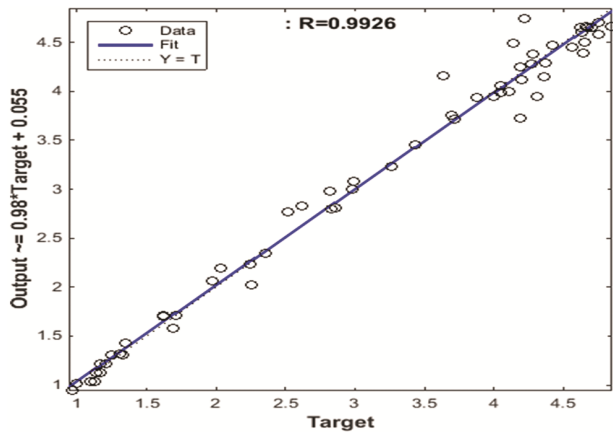
Fig. 5 — Regression plot for Curvelet

experimental values. ANN-PSO technique is used to model the average roughness of the RGB, Gray level co-occurrence matrix and curvelet transforms. The average error obtained for RGB is 12.64, GLCM is 7.8 and Curvelet transforms is 3.5. Among these three, curvelet transform has showed the less average error percentage and regression graph is plotted by considering the roughness values.

Conclusions

Machine vision systems based on artificial intelligence (AI) are developed to map the intricate relationships between surface images texture features data of machined components, and minute variations in surface roughness. Complex intelligent ANN-PSO models are developed to aid the machining industry in automating surface roughness measurement from texture feature data such as RGB, GLCM, and curvelet transform. A comparison is made of the AI surface roughness assessment models' efficacy. The curvelet transform-based model showed to be accurate and intelligent with a least percentile error over GLCM and RGB. The proposed machine vision system can be used in Industry 4.0 by automating surface roughness measurement technique. Machine vision-based systems for roughness estimation are essential for future production, business operations, efficiency improvement, and cost reduction to a more significant extent in "Industry 4.0."

References

1 Zain A M, Haron H & Sharif S, Prediction of surface roughness in the end milling machining using artificial neural network, *Expert Syst Appl*, **37(2)** (2010) 1755–1768, https://doi.org/10.1016/j.eswa.2009.07.033.

2 Samtas G, Measurement and evaluation of surface roughness based on optic system using image processing and artificial neural network, *Int J Adv Manuf Technol*, **73** (2014) 353–364, https://doi.org/10.1007/s00170-014-5828-1.

3 Raju R S & Ramesh R, Image and vibration based mixed variable approach for machining performance estimation, *Int J Appl Eng Res*, **11(4)** (2016) 2646–2650.

4 Palani S & Natarajan U, Prediction and control of surface roughness in cnc end milling by machine vision system using artificial neural network based on 2D fourier transform, *Int J Adv Manuf Technol*, **54** (2011) 1033–1042, https://doi.org/10.1007/s00170-010-3018-3.

5 Agrawal A , Goel S, Rashid W B & Price M, prediction of surface roughness during hard turning of AISI 4340 steel (69 HRC), *Appl Soft Comput*, **30** (2015) 279–286, http://dx.doi.org/10.1016/j.asoc.2015.01.059.

6 Nathan D, Thanigaiyarasu G & Vani K, Study on the relationship between surface roughness of AA6061 alloy end milling and image texture features of milled surface, *Procedia Eng*, **97** (2014) 150–157, https://doi.org/10.1016/j.proeng.2014.12.236.

7 Cuka B, Cho M & Kim D, Vision-based surface roughness evaluation system for end milling, *Int J Comput Integ M*, **31**(2018)727–738, https://doi.org/10.1080/0951192X.2017.1407451.

8 Shahabi H H & Ratnam M M,Simulation and measurement of surface roughness via grey scale image of tool in finish turning, *Precis Eng*, **43** (2015) 146–153,http://dx.doi.org/10.1016/j.precisioneng.2015.07.004.

9 Srivani A & Anthony Xavior M, Investigation of surface texture using image processing techniques, *Procedia Eng*, **97** (2014) 1943–1947,https://doi.org/10.1016/j.proeng.2014.12.348.

10 Patwari Md A U, Arif M D, Chowdhury Md S I & Chowdhury Md N A, Identifications of machined surfaces using digital image processing, *Int J Eng*, **X** (2012) 213–218.

11 Jurevicius M, Skeivalas J & Urbanavicius R, Analysis of surface roughness parameters digital image identification, *Measurement*, **56** (2014) 81–87, doi: http://dx.doi.org/10.1016/j.measurement.2014.06.005.

12 HuaianY I, Jian L I U, Enhui L U & Peng A O, Measuring grinding surface roughness based on the sharpness evaluation of colour images, *Meas Sci Technol*, **27** (2016), http://iopscience.iop.org/0957-0233/27/2/025404.

13 To W, Paul G & Liu D, Surface-type classification using RGB-D, *Autom Sci Eng*, **11** (2014) 359–366, doi: 10.1109/TASE. 2013.2286354.

14 Zhang Z, Chen Z, Shi J, Jia F & Dai M, Surface roughness vision measurement in different ambient light conditions, *Int J Comput Appl Technol*, **39(1-3)** (2008) 53–57, https://doi.org/10.1109/MMVIP.2008.4749497.

15 Dutta S, Datta A, Das Chakladar N, Pal S K, Mukhopadhyay S & Sen R, Detection of tool condition from the turned surface images using an accurate grey level co-occurrence technique, *Precis Eng*, **36** (2012) 458–466, doi:10.1016/j.precisioneng.2012.02.004.

16 Gadelmawla E S, Estimation of surface roughness for turning operations using image texture features, *J Eng Manuf*, **225(8)** (2011) 1281–1292, doi: 10.1177/ 2041297510393643.

17 Simunovic G, Svalina I, Simunovic K, Saric T, Havrlisan S &Vukelic D, Surface roughness assessing based on digital image features, *Adv Prod Eng Manag*, **11** (2016) 93–104. http://dx.doi.org/10.14743/apem2016.2.212.

18 Sun W, Yao B,Chen B, He Y, Cao X, Zhou T & Liu H, Noncontact surface roughness estimation using 2D complex

wavelet enhanced resnet for intelligent evaluation of milled metal surface quality, *Appl Sci*, **8** (2018) 381–405, doi:10.3390/app8030381.

19 Pour M, Determining surface roughness of machining process types using a hybrid algorithm based on time series analysis and wavelet transform, *Int J Adv Manuf Technol,* **97** (2018) 2603–2619, https://doi.org/10.1007/ s00170-018-2070-2.

20 Shen L & Yin Q, Texture classification using curvelet transform, *Int Symp Info Proc (ISIP'09)* (), 2009, 319-324.

21 Raju RS , Raju V R & Ramesh R, Curvelet transform for estimation of machining performance, *Optik*, **131** (2016) 615–625, http://dx.doi.org/10.1016 /j.ijleo.2016.11.181.

22 Raju R S, Ramesh R, Raju V R & Sharfuddin Md, Curvelet transforms and flower pollination algorithm based machine vision system for roughness estimation, *J Opt*, **47 (**2018) 243–250, https://doi.org/10.1007/s12596-018-0457-y.

23 Kaladhar M, Sameer Chakravarthy V S S & Chowdary P S R, Prediction of surface roughness using a novel approach, *Int J Ind Eng Prod Res*, **32(3)** (2021) 1–13, doi:10.22068/ ijiepr.32.3.1.

24 Raju R S, Sameer Chakravarthy V S S & Chowdary P S R, Flower pollination algorithm based reverse mapping methodology to ascertain operating parameters for desired surface roughness, *Evol Intell*, **14** (2021) 1145–1150, https://doi.org/10.1007/s12065-021-00574-1.